DOT/FAA/TC-13/20

Federal Aviation Administration
William J. Hughes Technical Center
Aviation Research Division
Atlantic City International Airport
New Jersey 08405

Development of Technologies to Improve the Reliability and Intelligence of Aircraft Electrical Wiring Interconnection Systems

November 2013

Final Report

This document is available to the U.S. public through the National Technical Information Services (NTIS), Springfield, Virginia 22161.

This document is also available from the
Federal Aviation Administration William J. Hughes
Technical Center at actlibrary.tc.faa.gov.

U.S. Department of Transportation
Federal Aviation Administration

NOTICE

This document is disseminated under the sponsorship of the U.S. Department of Transportation in the interest of information exchange. The U.S. Government assumes no liability for the contents or use thereof. The U.S. Government does not endorse products or manufacturers. Trade or manufacturers' names appear herein solely because they are considered essential to the objective of this report. The findings and conclusions in this report are those of the author(s) and do not necessarily represent the views of the funding agency. This document does not constitute FAA policy. Consult the FAA sponsoring organization listed on the Technical Documentation page as to its use.

This report is available at the Federal Aviation Administration William J. Hughes Technical Center's Full-Text Technical Reports page: actlibrary.tc.faa.gov in Adobe Acrobat portable document format (PDF).

Technical Report Documentation Page

1. Report No.	2. Government Accession No.	3. Recipient's Catalog No.
DOT/FAA/TC-13/20		

4. Title and Subtitle	5. Report Date
DEVELOPMENT OF TECHNOLOGIES TO IMPROVE THE RELIABILITY AND INTELLIGENCE OF AIRCRAFT ELECTRICAL WIRING INTERCONNECTION SYSTEMS	November 2013
	6. Performing Organization Code
7. Author(s) Robert Kauffman	8. Performing Organization Report No.
9. Performing Organization Name and Address University of Dayton Research Institute 300 College Park Dr. Dayton, OH 45469-0161	10. Work Unit No. (TRAIS)
	11. Contract or Grant No. Grant: 11-G-011
12. Sponsoring Agency Name and Address U.S. Department of Transportation Federal Aviation Administration Northwest Mountain Region—Transport Airplane Directorate 1601 Lind Avenue, SW Renton, WA 98057	13. Type of Report and Period Covered Final Report August 2011 – August 2012
	14. Sponsoring Agency Code ANM-111

15. Supplementary Notes

The Federal Aviation Administration William J. Hughes Technical Center Aviation Research Division Technical Monitor was Michael Walz.

16. Abstract

This report details the results of a 12-month research program performed by the University of Dayton Research Institute to improve the reliability and intelligence of aircraft electrical wiring interconnection systems (EWIS) through improved malfunction detection. The research was performed to develop radio frequency identification tag-based sensors that are activated by abnormal operating conditions prior to EWIS or associated component failure. The sensors were designed to detect improper clamp installation, clamp breakage, unsupported wire harness impacts with structures, thermal events, chemical attacks, loss of power, and component fatigue/cracks.

17. Key Words	18. Distribution Statement
Electrical wiring interconnect systems, Radio frequency identification tag, Wireless sensors, Condition monitoring	This document is available to the U.S. public through the National Technical Information Service (NTIS), Springfield, Virginia 22161. This document is also available from the Federal Aviation Administration William J. Hughes Technical Center at actlibrary.tc.faa.gov.

19. Security Classif. (of this report)	20. Security Classif. (of this page)	21. No. of Pages	22. Price
Unclassified	Unclassified	36	

TABLE OF CONTENTS

		Page
EXECUTIVE SUMMARY		viii
1.	SMART SENSOR DESIGN AND PRODUCTION	1
1.1	Passive RFID Tags	1
1.2	Modified Passive RFID Tag	2
1.3	Production of Modified High Frequency RFID Tag	3
1.4	Modified High Frequency RFID Tags With Remote IC Bypass	4
1.5	Modified Low Frequency RFID Tags With Remote IC Bypass	6
2.	SMART CLAMP SENSOR	8
3.	SMART THERMAL SENSOR	10
4.	SMART CHEMICAL SENSOR	13
5.	SMART IMPACT SENSOR	19
6.	SMART POWER SENSOR	25
7.	SMART CRACK SENSOR	26
8.	CONCLUSIONS	26
9.	REFERENCES	27

LIST OF FIGURES

Figure		Page
1	Alien GEN 2 Squiggle RFID Tag	1
2	Construction of SMART Clamp Sensor Based on UHF RFID Tag	2
3	Production Drawing for HF RFID Tag With IC Bypass	3
4	Sheet of Modified HF RFID Tags and Single-Tag Detailing Components	4
5	Modified HF RFID Tag With Wires Attached to the IC Bypass	5
6	Modified HF and Commercial LF RFID Tags	7
7	Different Locations for Monitoring Clamp Status	9
8	SMART Clamp Sensors Using Push-Button and Thin Film Switches to Complete the IC Bypass	9
9	SMART Clamp Sensor Using a Remote Metal-to-Metal Connection to Complete the IC Bypass	10
10	Copper Pads on Polyimide Sheets Used to Evaluate Different Paraffin Wax/Silver Metal Mixtures for Use in a Meltable IC Bypass	11
11	SMART Thermal Sensor Using a Remote Field's Metal Wire Connection to Complete the IC Bypass	12
12	SMART Chemical Sensor Using a Vapor-Deposited Copper Film to Complete the IC Bypass	13
13	Glass Slide Pieces With Tin, Aluminum, and Copper Metal Films Before and After Exposure to HFA Vapors	14
14	Glass Slide Pieces With Different Metal Films Before and After Exposure to Corrosive Vapors and Aqueous Solutions	15
15	SMART Chemical Sensors Completed by Aluminum and Tin Metal Films After Exposure to HFA Vapors	16
16	SMART Chemical Sensor Completed With Silver Epoxy Line After Exposure to HFA Vapors	17

17	SMART Chemical Sensor Completed With Silver Metal Film After Exposure to HFA Vapors	17
18	SMART Chemical Sensor Using a Conductive Silicone Rubber Cord to Complete the IC Bypass	18
19	Cross-Sectioned Normally Closed G-Switch	20
20	One-Time Use Shipping Sensor Based on Spring/Ball Concept	21
21	Ball/Spring Combination Falling Apart After Acceleration	21
22	Unsupported Wire Bundle With Wireless and Ball/Spring Accelerometers Attached for Monitoring Structure Impacts	22
23	SMART Impact Sensor Using a Tilt Sensor (Cross-Section Insert) to Complete the IC Bypass	24
24	Experimental Setup for Determining Weight Required to Break Scribed Alumina Slide	24
25	SMART Power Sensor Using a Reed Switch to Complete the IC Bypass	25

LIST OF TABLES

Table		Page
1	Comparison of Different RFID Tag Technologies	1
2	Effects of the IC Bypass Resistance on the Maximum Read Range of a Modified HF RFID Tag	6
3	Effects of the IC Bypass Resistance on the Maximum Read Range of a Commercial LF RFID Tag	8
4	Data Generated by Different Accelerometers Attached to Unsupported Wire Bundle During Shaking and Impact Motions	23

LIST OF SYMBOLS AND ACRONYMS

Ω	Ohms
KΩ	Kiloohms
MΩ	Megaohms
EWIS	Electrical wiring interconnection systems
g	Acceleration of gravity
HF	High frequency
HFA	Hydrofluoric acid
HCl	Hydrochloric acid
IC	Integrated circuit
KAc	Potassium acetate
KOH	Potassium hydroxide
LF	Low frequency
NaCl	Sodium chloride
RFID	Radio frequency identification
SMART	Status and Motion-Activated Radiofrequency Tag
UDRI	University of Dayton Research Institute
UHF	Ultra high frequency

EXECUTIVE SUMMARY

The electrical wiring interconnection system (EWIS) of an aircraft uses miles of complex networks of electrical wiring, connectors, clamps, etc. to carry general electrical power, electrical signals for operating components, and communication signals. During the lifetime of an aircraft, the different components of the EWIS experience a wide range of physical and chemical stresses; vibration, abrasion, hydrolysis, fatigue, thermal decomposition, and chemical reactions combine to degrade the insulation of wiring and connectors. Polyimide-type wiring insulations, present in many older aircraft EWIS, are especially susceptible to hydrolytic and chemical degradation reactions. Once degradation of the wiring insulation allows the ingression of moisture, chemicals, and gaseous pollutants, the resulting corrosion of the metallic conductors and connectors increases the potential for control malfunctions, dry and wet arcing, conduit burn-through, and damage to control cables and linkages. The metallic conductors of the electrical wiring and connectors experience low- and high-cycle fatigue, eventually leading to partial and complete breaks in the wiring and fretting wear/surface separation in the connectors. The increase in connector resistance due to corrosion and metal surface separation further reduces the signal-to-noise ratios in low-power avionics and increases the risk of local heating and fire hazards in high-power circuits.

Consequently, the potential safety hazards resulting from insulation damage, conductor breakage, connector deterioration, excessive vibration due to clamp breakage, for example, require that immediate maintenance actions be taken to ensure reliable EWIS performance. However, the miles of inaccessible, bundled, branched wiring of aircraft EWIS, and the fact that many of the failure mechanisms can best be detected while the EWIS is powered, greatly reduces the effectiveness of malfunction detection and repair technologies currently in use today. Therefore, a research program focused on the development and evaluation of wireless sensors based on modified radio frequency identification (RFID) tags has been performed to improve the reliability and intelligence of aircraft EWIS.

The modified RFID sensors developed during this project were designed based on the concept of condition-based activation (i.e., even though thousands of sensors are present on an aircraft, only the sensors experiencing an abnormal condition will output a signal). Because the activated sensor outputs information on the type and location of the abnormal condition, simple readers/data handling systems can be used by maintenance personnel to locate/identify the malfunction with minimal effort and effect on surrounding EWIS components. Therefore, the condition-based sensors are referred to as Status and Motion-Activated Radiofrequency Tag (SMART) sensors.

During this project, passive SMART sensors were developed to detect a wide range of EWIS abnormal conditions. The sensors were designed to detect improper clamp installation, clamp breakage, unsupported wire harness impacts with structures, thermal events, different chemical attacks, loss of power, and component fatigue/cracks.

1. SMART SENSOR DESIGN AND PRODUCTION.

Based on the Status and Motion Activated Radiofrequency Tag (SMART) clamp concept investigated during the previous research project [1], SMART sensors have been designed for detecting a wide range of abnormal operating conditions in new and aging aircraft electrical wiring interconnection systems (EWIS) prior to component failure. The SMART sensors have two primary components: a radio frequency identification (RFID) tag and a sensing element that changes state to detect improperly installed or broken clamps/ties, unsupported wiring harnesses striking against structures, corrosive gases/liquids, thermal events (temperature, combustion products, etc.), loss of power, and cracks in polymeric surfaces.

1.1 PASSIVE RFID TAGS.

There are generally two types of RFID tags: active RFID tags, which contain a battery and can transmit signals continuously without exterior prompting; and passive RFID tags, which have no battery and require an external source (an interrogator/reader) to activate the tag and read the stored information. The main advantage of the active RFID tags compared to the passive tags is their longer read range. However, the requirement of a battery (even printed batteries or energy-scavenging systems, such as those from Cymbet™, Elk River, MN) increases the weight, cost, and complexity of the tag modified for use in the SMART sensors. Consequently, passive RFID tags were the primary focus of the project to develop SMART sensors.

Several types of passive RFID tags suitable for development into a SMART sensor are commercially available. As summarized in table 1, there are three main frequency ranges used by commercial RFID tags.

Table 1. Comparison of Different RFID Tag Technologies

RFID Tag	Frequency	Read Range	Antenna	Reprogrammable
Low Frequency (LF)	125 KHz	< 1 foot	Coil	Varies
High Frequency (HF)	13.56 MHz	< 1 foot	Trace	Yes
Ultra HF (UHF)	850 – 950 MHz	20+ feet	Trace	Yes

Passive RFID tags have three main components: integrated circuit (IC), antenna (A1 and A2 with connecting copper metal trace), and substrate (paper backing with plastic coating) as depicted on the ultra high frequency (UHF) GEN 2 Squiggle® RFID tag manufactured by Alien Technology® (Dayton, OH), shown in figure 1.

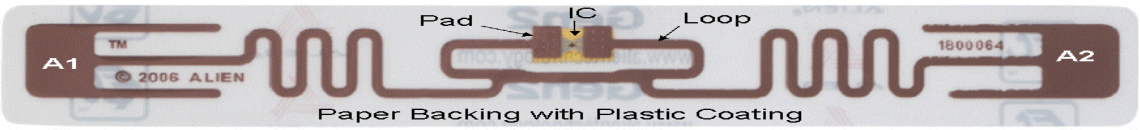

Figure 1. Alien GEN 2 Squiggle RFID Tag [1]

The GEN 2 Squiggle RFID tag is well suited for incorporation into the SMART sensors because of its size (97 mm by 11 mm), weight (<0.2 grams), cost (currently $0.30), accessibility of IC circuit, and reprogrammability (e.g., for SMART clamp sensors, have the tag output C1 for clamp 1, C2 for clamp 2, etc.). The flexible RFID tag has a paper backing that is coated with a thin layer of clear plastic to protect the copper traces from corrosion, and an adhesive surface that is adhered to clamps and other surfaces to be monitored. Consequently, it was the first tag evaluated for development into the SMART sensor technology [1].

1.2 MODIFIED PASSIVE RFID TAG.

The SMART sensor is based on the concept that the sensor is activated by the initiation of an abnormal operating condition (e.g., clamp breaks, impact, hot spot). In the case of a passive RFID tag-based sensor, the RFID tag will not be detectable/readable when the monitored condition is normal. When an abnormal condition occurs, the UHF RFID tag is readable by a proximate reader so that the identification information encoded into the IC of the tag can be used to locate the failed component, abnormal condition, etc.

Of the various passive tag modifications previously studied, the optimum method of reversible deactivation was achieved by adding an electrical bypass to the IC circuitry [1 and 2]. Based on the GEN 2 Squiggle RFID tag design (figure 1), an RFID tag was etched on a polyimide circuit board incorporating the IC bypass concept, as shown in figure 2.

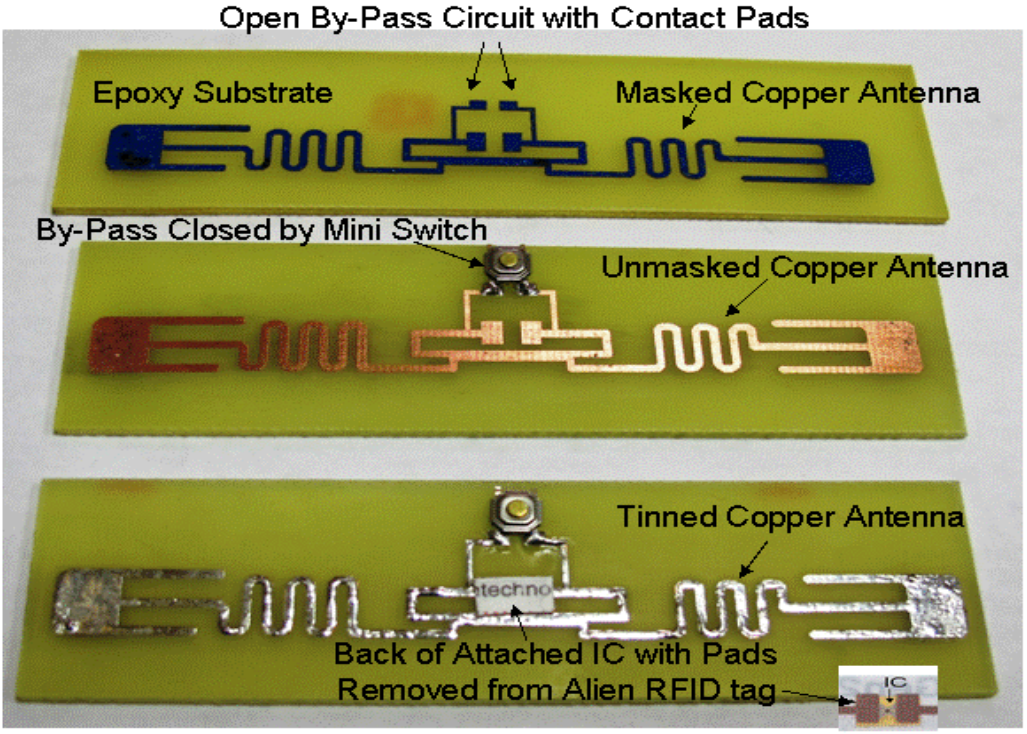

Figure 2. Construction of SMART Clamp Sensor Based on UHF RFID Tag

An IC cut from an Alien tag was then adhered to the loop pads of the etched antenna in figure 2 to give the prototype SMART sensor memory. With a push-button switch in the IC bypass circuit, the IC was deactivated (the tag was unreadable) when the switch was pushed/closed and was activated when the switch was released/opened (the tag was readable).

Because the optimum passive SMART sensor design incorporates an IC bypass, the SMART sensor technology could be used to monitor different EWIS components for abnormal operating conditions by using the following sensing elements in the IC bypass:

- Clamp (push-button switch, separable contacts)
- Thermal event arcing (meltable trace/substrate)
- Chemical exposure (corrodible trace, conductive polymer)
- Impact by unsupported wires (g-switch, fragile trace)
- Remote-powered device (reed switch)
- Crack (brittle trace broken by impact, fatigue, wear, etc.)

1.3 PRODUCTION OF MODIFIED HF RFID TAG.

Since a commercial RFID tag was needed for the SMART sensor evaluation for the different abnormal operating conditions, the initial focus of the project was working with American Thermal Instruments (Dayton, OH, SMART technology licensee) to design (see figure 3) and mass produce a high frequency (HF) RFID tag with the required IC bypass.

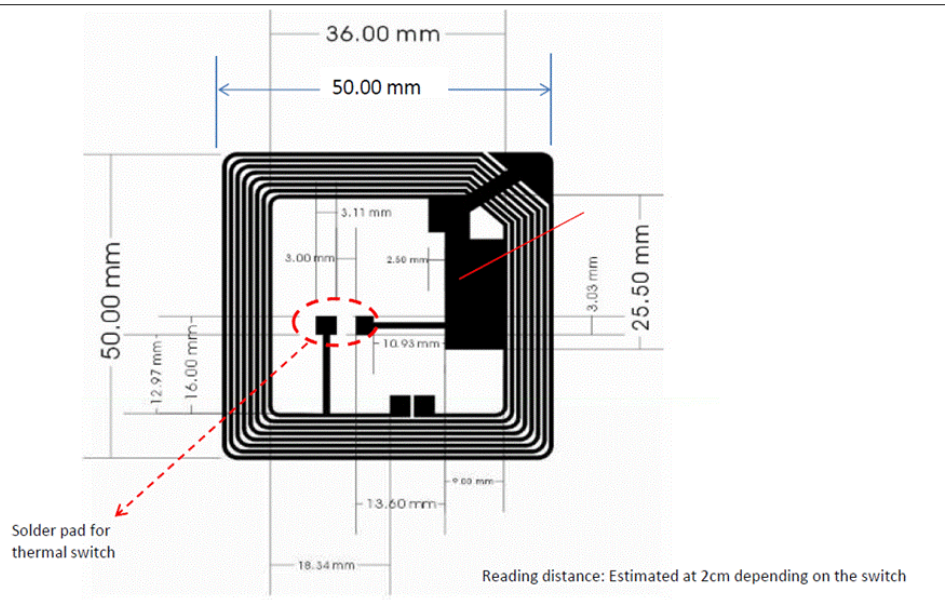

Model Name	13.56MHz HF customized Tag	Approve
Model No.		
IC chip	NXP I-Code 1024bit	
Track Material	Aluminium	
Solder pad	Tinted Lead	
Bottom layer	Adhesive	
Packaging	10k roll	Date:

Figure 3. Production Drawing for HF RFID Tag With IC Bypass

The HF (13.56 MHz) RFID tag was selected for mass production because the antenna design is widely used and has no patent infringement concerns (UHF antenna/tag design in figures 1 and 2 is an Alien Technology design). The RFID tag was designed with an aluminum antenna to minimize the weight and cost of the tag, and solder pads were added to the IC bypass for connecting the selected switch/trace. The read range of the HF tag was predicted to be 0.8 inch (typical for HF RFID tags), which was suitable for demonstrating the different applications of the SMART sensor technology.

A production run of 10,000 modified tags was made by printing the modified HF RFID tags four-wide on a 30-cm-wide roll of plastic film (polybutylene terephthalate), based on the drawing in figure 3, a section of the plastic film containing 16 modified tags with the printed RFID tags and a single RFID tag is shown in figure 4.

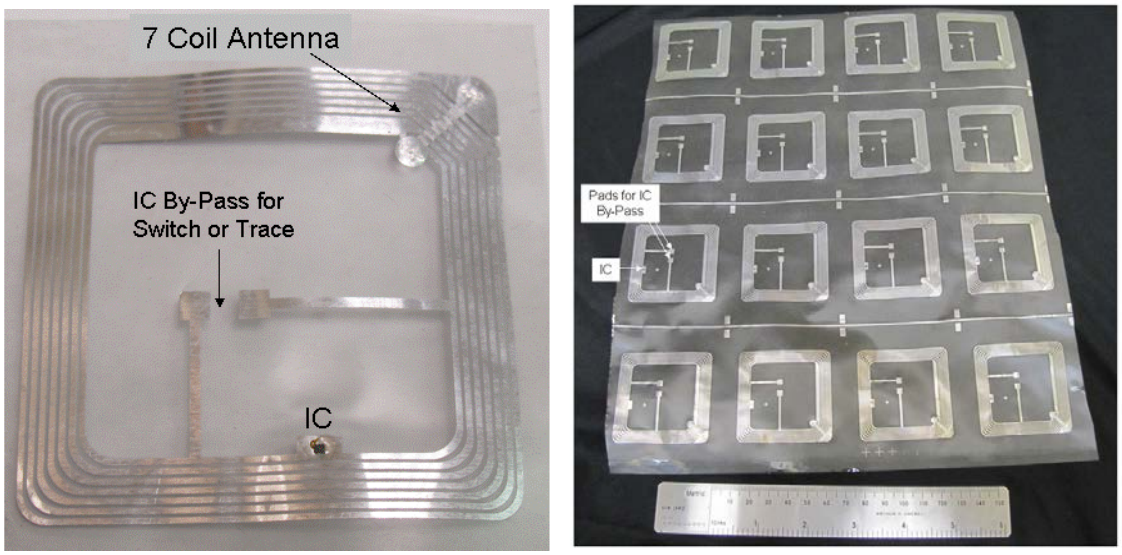

Figure 4. Sheet of Modified HF RFID Tags and Single-Tag Detailing Components

The HF RFID tags in figure 4 could be read up to 0.8 inch (as predicted) through air and through 0.8-inch-thick sheets of high-density polyethylene and an acrylic sheet with an electrostatic coating. However, the HF RFID tags could not be read through a 0.8-inch-thick carbon fiber composite panel (electrical compartment door, outside aircraft wall, etc.). The HF tag read range was up to 0.2 inch when reading through carbon fiber laminates.

1.4 MODIFIED HIGH FREQUENCY RFID TAGS WITH REMOTE IC BYPASS.

Due to the limited read range of the HF RFID tags, the potential for attaching electrical wires to the IC bypass was studied to allow the incorporated switch to be placed remotely from the RFID tag. Figure 5 shows 22-gauge wires attached with silver epoxy to the pads of the IC bypass and small alligator clips added to the opposite ends of the wires to attach various switches and different lengths of a conductive silicone rubber cord to the wires.

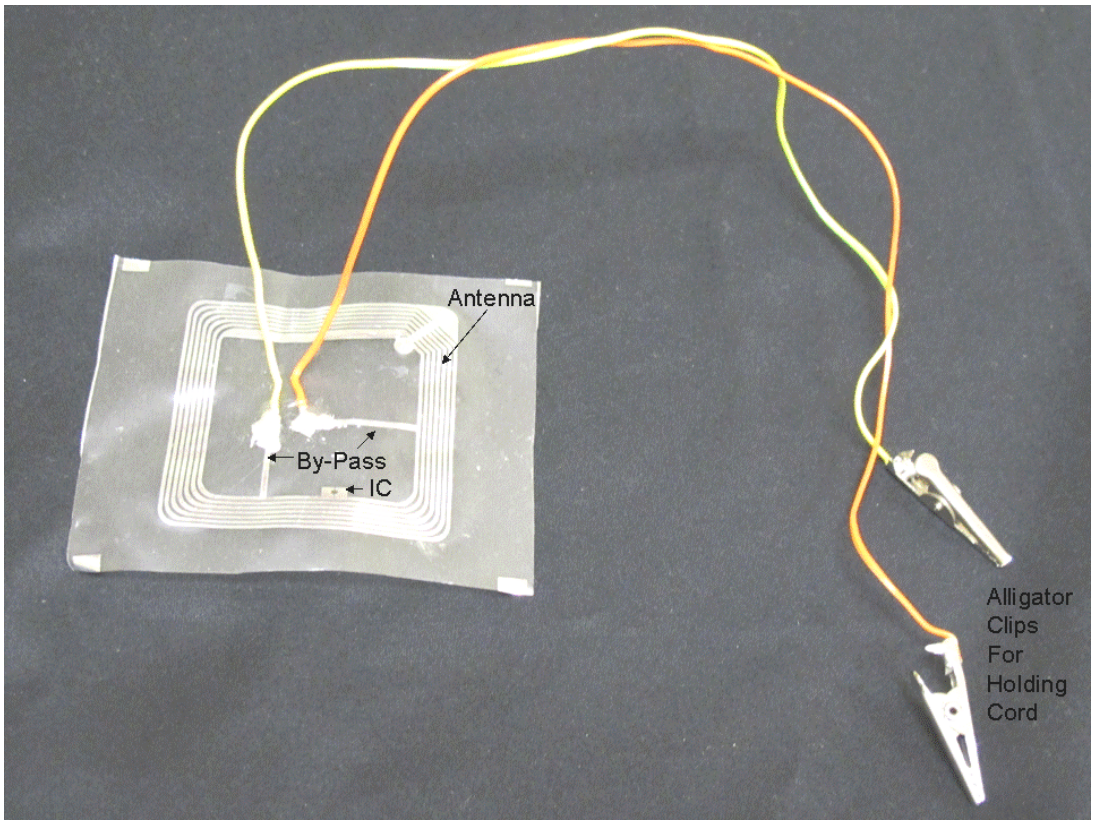

Figure 5. Modified HF RFID Tag With Wires Attached to the IC Bypass

As long as the attached wires were not pressed against the uncoated aluminum antenna, the attachment of the wires had no effect on the read range of the RFID tag until the clips were connected (circuit closed, tag unreadable). The read range of the modified UHF RFID tags (commercial or University of Dayton Research Institute prototype) was not significantly affected when the wires were attached to the IC pad bypass (figure 2) of the tags. However, in contrast to the HF tags, when the clips touched, the readability of the tag was not affected (it was later determined that the attached wires acted like a secondary antenna).

To determine the effects of the bypass resistance on the maximum read range of the modified HF RFID tag, the alligator clips (figure 5) were attached to increasing lengths of a conductive silicone cord. As the length of cord between the two alligator clips was increased from 0 (clips touching) to 10 inches, the resistance of the IC bypass increased from <1 ohm (Ω) to 5 kiloohms (KΩ). The cord length between the two alligator clips, the resistance of the cord between the two alligator clips (IC bypass resistance), and the maximum distance from which the HF RFID tag could be read are listed in table 2.

Table 2. Effects of the IC Bypass Resistance on the Maximum Read Range of a Modified HF RFID Tag

Cord length (inches)	IC Bypass Resistance (KΩ)	Maximum Read Distance (inches)
0	(<1 Ω)	0
0.5	0.32	0
1	0.63	0
1.5	0.82	0
2	1.06	0.25
3	1.62	0.50
4	2.17	0.50
5	2.55	0.50
6	3.00	0.625
7	3.40	0.625
10	4.90	0.75
No cord	Open	0.75

As listed in table 2, the HF RFID tag was unreadable when the IC bypass resistance was below 1 KΩ (even when laid directly on the reader). From 1 to 5 KΩ, the maximum distance from which the tag could be read increased slowly with IC bypass (cord) resistance. There was no difference in the maximum read distance of the tag above 5 KΩ (the same maximum read distance as the modified tag with open bypass or commercial HF tags). These results indicate that, as long as the IC bypass resistance is below 1 KΩ, the bypass will act as an on/off switch (minimizing the need for reader calibration for different environments).

If the IC bypass resistance is between 1 and 5 KΩ, the maximum read distance could be used to trend an ongoing process (commercial readers with read distance determination capability are available). For example, for a SMART chemical sensor, the maximum read distance could be used to monitor the corrosion of a metal film completing the IC bypass (resistance increases 1 Ω to 5 KΩ as film is dissolved/chemically attacked by corrosive gas/liquid). Because the maximum read distance is affected by the environment, the reader would have to be standardized for the intended environment and would require periodic recalibrations to ensure the accuracy of the distance determinations.

1.5 MODIFIED LOW FREQUENCY RFID TAGS WITH REMOTE IC BYPASS.

Because of the limited read range of the HF RFID tags through carbon fiber composite panels, the potential for attaching wires to the IC of commercial low frequency (LF) RFID tags was also studied. The LF tags were investigated because they can be read through thicker, more conductive substrates (e.g., 0.8-inch-thick carbon composite panel) than the HF tags. To obtain access to the metallic pads holding the IC in place and associated metal coil antenna, the outer

layers of two plastic cards LF RFID tags were peeled back. Figure 6 shows the exposed IC, the antenna of the LF tags, and a pair of modified HF RFID tags (included for size comparison).

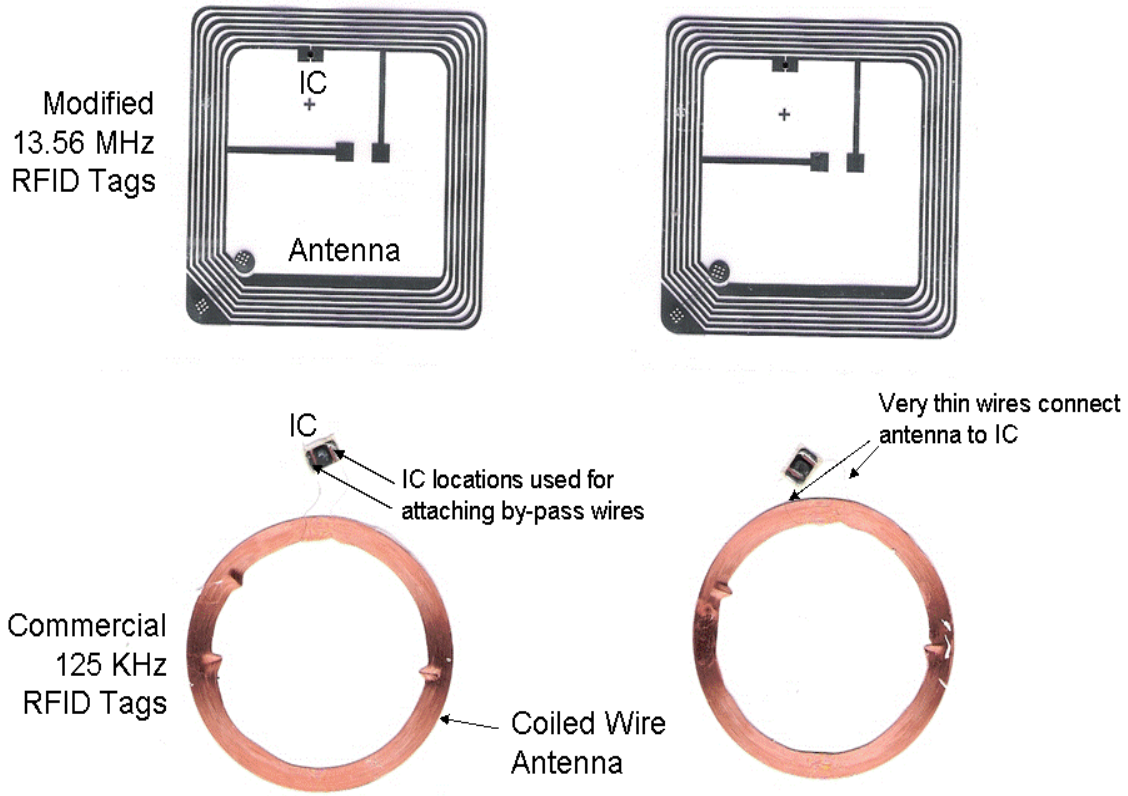

Figure 6. Modified HF and Commercial LF RFID Tags

To determine if the maximum read range of LF RFID tags could be affected by an IC bypass (as listed in table 2 for the modified HF RFID tags), 22-gauge wires were electrically attached (silver epoxy) to the solder pads of the exposed ICs and small alligator clips were added to the opposite ends of the wires. When the alligator clips were touched together (circuit closed), the LF tag could not be read. Similar results were obtained when the alligator clips were attached to opposite sides of a push-button switch (i.e., switch open: RFID tag could be read; switch closed: RFID tag could not be read). Consequently, the LF RFID tag could be used to monitor proximate as well as remote switches/sensors (the same as the HF RFID tags). However, in contrast to the higher frequency (13.56 MHz) HF RFID tags, the LF RFID (125 KHz) tags could be read through a thick composite panel (electrical compartment door, outside aircraft wall, etc.).

To determine the effects of the IC bypass resistance on the read range of the LF RFID tags, the alligator clips were attached to increasing lengths of a conductive silicone cord (carbon black, 1/8-inch OD). As the cord length between the two alligator clips increased from 0 (clips touching) to 24 inches, the resistance of the bypass increased from <1 Ω to 10 KΩ. The cord length between the two alligator clips, the resistance of the cord between the two alligator clips (the IC bypass resistance), and the maximum distance from which the LF RFID tag could be read are listed in table 3.

Table 3. Effects of the IC Bypass Resistance on the Maximum Read Range of a Commercial LF RFID Tag

Cord length (inches)	IC Bypass Resistance KΩ	Maximum Read Distance (inches)
0	0	0
2	1.2	0
3	1.4	1/8
4	1.8	1/4
5	2.3	1/4
6	2.75	1/2
8	3.5	1/2
10	4.3	1/2
12	5.2	1/2
18	7.6	3/4
24	9.8	1
No Cord	Open	1

As shown in table 3, the LF RFID tag was unreadable (laid on reader: 0 inches) when the IC bypass resistance was below 1 KΩ (similar to the HF results in table 2). From 1 to 10 KΩ, the maximum distance from which the tag could be read increased slowly with the IC bypass (cord) resistance. There was no difference in the maximum read distance of the tag above an IC bypass resistance of 10 KΩ (the HF RFID tag reached its maximum read distance at a lower IC bypass resistance of 3 KΩ). These results indicate that, as long as the HF tag bypass resistance is below 1 KΩ, the bypass will act as an on/off switch. However, if the bypass resistance is between 1 and 10 KΩ, the read distance could be used to trend an ongoing process. For example, the corrosion sensor could trend corrosion of metal film connected to IC (resistance increases from 1 Ω to 10 KΩ as film attacked by corrosive gas/liquid) or the clamp sensor with pressure-sensitive film could detect the clamp starting to open.

2. SMART CLAMP SENSOR.

Although it was investigated thoroughly in the previous project [1], additional work was performed developing a SMART clamp sensor based on the modified HF RFID tags in figure 4. The pressure-sensitive elements investigated for use in the IC bypass were miniature push-button switches [1], thin film pressure pads, and copper films applied to inner clamp surfaces (metal-to-metal contact when the clamp closed). Thin film sensors with a pressure-sensitive pad suitable for detecting clamp status at different clamp locations were identified at the SENSORS Tech Forum in October 2011 [3] and at rocket hobby websites. The clamp locations identified for the placement of the pressure-sensitive elements are shown in figure 7 as: A (clamp opening), B (loss of harness due to the clamp breaking), and C (clamp opening/clamp separation from the structure).

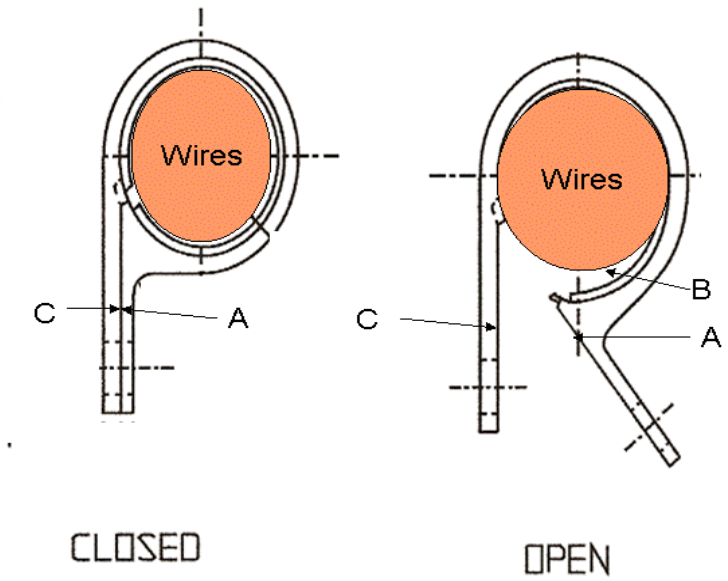

Figure 7. Different Locations for Monitoring Clamp Status

The resistance of the pressure-sensitive pad (measured at the electrical leads) was greater than 600 KΩ when no pressure was applied (clamp open/closed improperly/failed, RFID tag readable), but increased with finger pressure to less than 1KΩ (clamp closed properly, RFID tag unreadable). Figure 8 shows pictures of the RFID tags with the flexible, pressure-sensitive pad and miniature push-button switch attached directly to the IC bypass pads using silver epoxy.

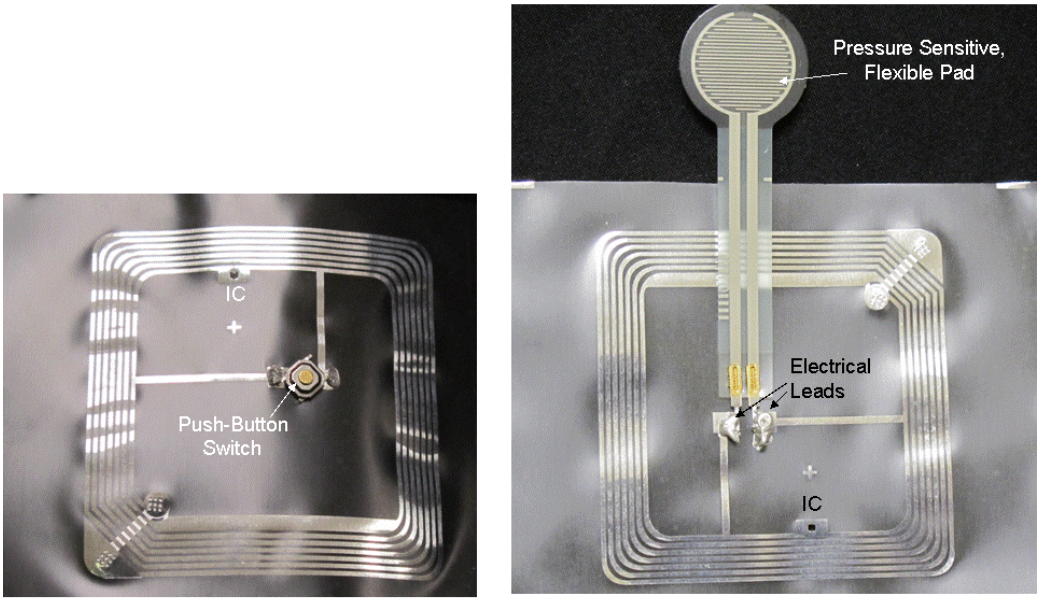

Figure 8. SMART Clamp Sensors Using Push-Button and Thin Film Switches to Complete the IC Bypass

In addition to attaching a switch or pad directly to the IC bypass of the modified HF RFID tags in figure 8 (requires that the RFID tag be placed in/next to clamp), two wires were attached to the IC bypass pads (silver epoxy). The other ends of the wires were then connected (silver epoxy) to two copper films adhered to an aircraft nylon clamp (locations A and C in figure 7), as shown in figure 9. Nonconductive epoxy was added to the clamp and RFID connections for improved ruggedness during repeated testing.

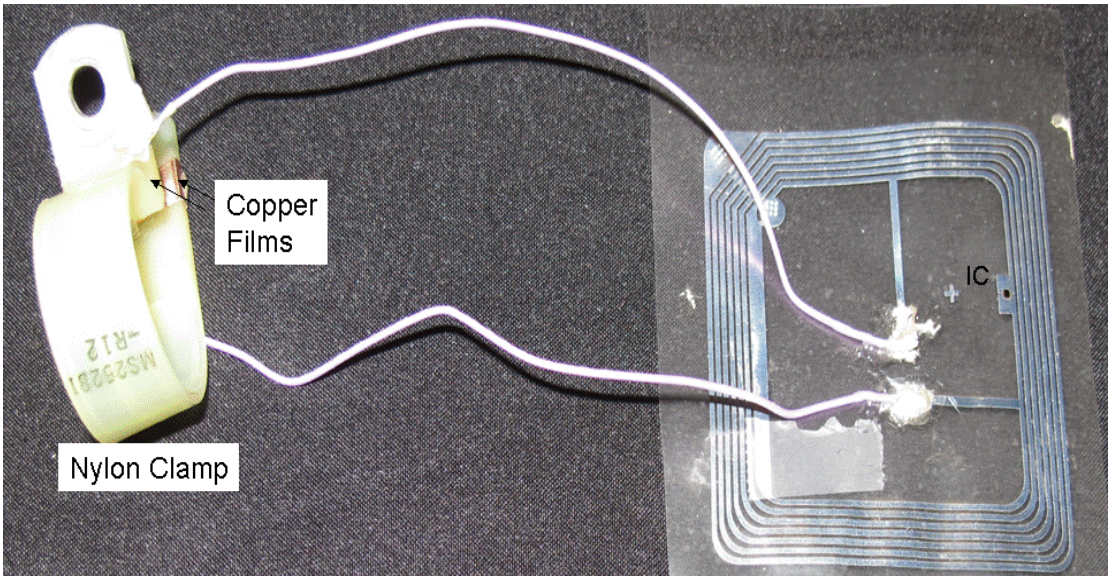

Figure 9. SMART Clamp Sensor Using a Remote Metal-to-Metal Connection to Complete the IC Bypass

According to the data in tables 2 and 3, the length of the wires connecting the RFID tag to the clamp can be as long as needed (wire resistance insignificant), so that an RFID tag placed on the back of an access panel can be connected to a remote, inaccessible clamp. By keeping the total resistances below 1 KΩ, multiple clamps wired in series can be monitored by a single remote RFID tag. Consequently, SMART sensors based on either LF or HF RFID tags can be used to monitor the status/health of multiple, remote clamps without opening the access panel/climbing through stacks of wiring harnesses. With further refinement/calibration of both the reader and the pressure-sensitive pad, the SMART clamp sensor has the potential for detecting clamps that are just starting to loosen by detecting changes in the maximum read range of the associated RFID tag (read range decreases with pressure between resistances of 2 and 10 KΩ; see tables 2 and 3)

3. SMART THERMAL SENSOR.

The following methods were investigated for making a temperature-sensitive IC bypass for the SMART thermal sensor:

- Meltable, conductive trace on RFID substrate
- Conductive trace on a low-temperature melting wax
- Remote attachment of wire/rod of low-melting metal alloy

The meltable, conductive alloy studied in this project was Field's metal because it melts at 62°C (144°F) and is a eutectic alloy of bismuth 32.5%, indium 51%, and tin 16.5% (does not contain lead or cadmium). Paraffin waxes with different melting points ranging from 50 to 85°C (122 to 185°F) were used to both supply a low-melting substrate and provide surface adhesion for a conductive trace made from silver metal powder. Field's metal and paraffin waxes were selected for this project because of their availability and low temperature range for demonstrating the potential of the SMART thermal sensor. The application of the SMART thermal sensors (e.g., overheating components/wires, arcing events, fires) dictate the required activation temperature and, consequently, the meltable metal/polymer used in the IC bypass.

Since the IC solder connections and substrates of most commercial RFID tags have temperature limitations, the IC bypass pads of a SMART thermal sensor were simulated by etching two metal pads (posts added for making electrical contact because the pads oxidized over time) from copper-plated polyimide sheets, as shown in figure 10.

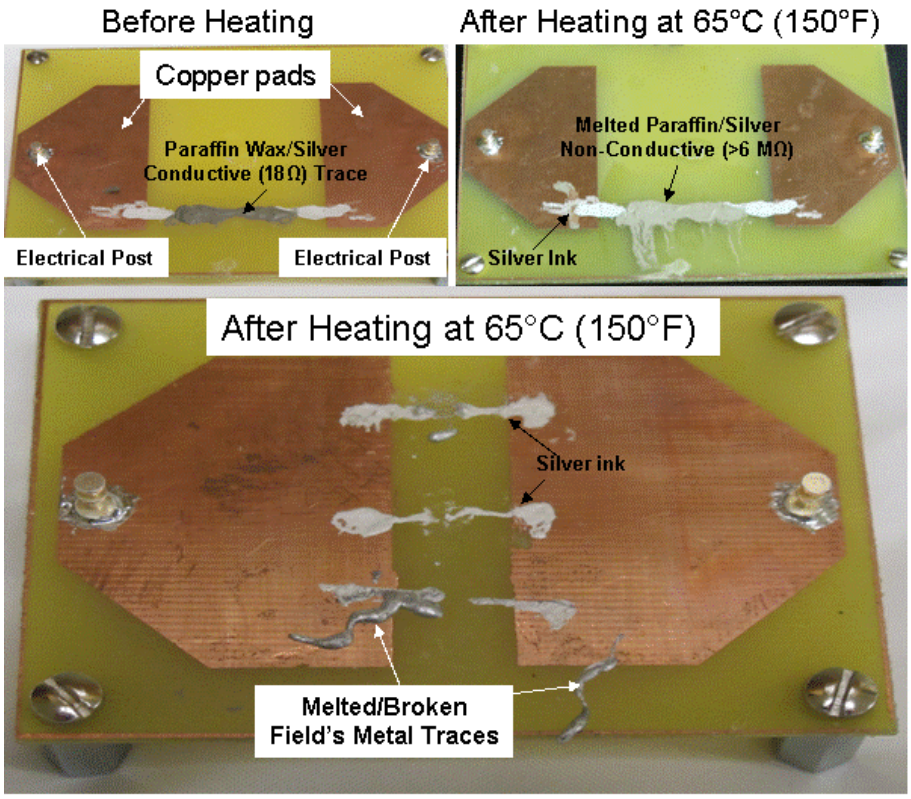

Figure 10. Copper Pads on Polyimide Sheets Used to Evaluate Different Paraffin Wax/Silver Metal Mixtures for Use in a Meltable IC Bypass

The first meltable trace investigated was a 50/50 mixture of low-molecular-weight paraffin wax (melt point = 55°C (131°F)) and 10 micron silver particles. The mixture was heated to 65°C (150°F) and the thick liquid was dispensed onto the polyimide surface to form a conductive trace between the adjacent ends of two silver ink traces, as shown in figure 10 (before heating). Silver ink traces were used to make the electrical contacts between the conductive trace and copper pads because the unprotected pads oxidized with time. After cooling, the liquid formed an

adherent, conductive trace (resistance = 18 Ω measured at electrical posts). When the board with the copper pads and paraffin trace was placed flat in an oven at 65°C (150°F) for 5 minutes, the paraffin wax melted, but the trace remained conductive as the silver particles settled/concentrated on the polyimide surface. However, when the board was placed vertical on its lower side (or was held horizontal and shaken while hot), the wax/silver particles flowed, as shown in figure 10 (after heating), and the trace opened (resistance >6 MΩ (megaohms)).

The second meltable trace investigated was a wire of Field's metal (melts at 62°C (144°F)). The wire was positioned on the polyimide board to complete the gap between the adjacent ends of the silver traces connected to the copper pads. A soldering iron was then used to melt/adhere the ends of the metal wire to the silver lines (resistance <1Ω measured at electrical posts). When the board with the copper pads and Field's metal wire was placed flat in an oven at 65°C (150°F) for 5 minutes, the wire melted/pooled, but the trace was conductive, remaining in contact with the silver ink lines. However, when the board was placed vertically on its lower side (or was held horizontally and shaken while hot), the melted wire softened and the trace was broken, but partially retained its shape, as shown in the lower portion of figure 10.

As shown in figure 9, the IC bypass element can be located far away from the RFID tag, allowing for the SMART thermal sensor to monitor temperatures well above the operating temperature of the RFID tag—the commercialized LF tag in figure 4 is limited by the melt point (~ 200°C (400°F)) of the plastic film substrate as well as the IC solder connections. Figure 11 shows a SMART thermal sensor with a Field's metal wire attached to two 22-gauge wires.

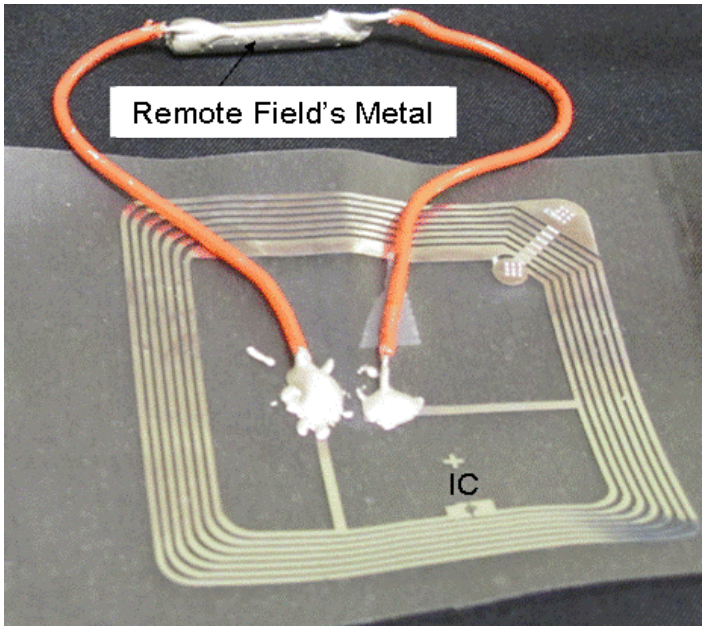

Figure 11. SMART Thermal Sensor Using a Remote Field's Metal Wire Connection to Complete the IC Bypass

As opposed to the wax/powder traces and Field's wire positioned on/supported by the polyimide circuit board in figure 10, when the Field's metal wire in figure 11 melted, it separated from the connecting wires (the RFID tag activated) independent of the RFID tag orientation or movement.

As with the SMART clamp sensor system, one SMART thermal sensor using an HF RFID tag placed on the back of a composite access panel could be read to detect excessive temperature events in one or multiple remote locations without having to open the panel or disturbing numerous EWIS.

4. SMART CHEMICAL SENSOR.

For a SMART chemical sensor to be effective, the conductive IC bypass would need to become nonconductive when exposed to a gas or liquid that was detrimental to aircraft EWIS. The two types of conductive bypasses studied for use in the SMART chemical sensor were vapor-deposited metal films (which became nonconductive because of corrosion) and conductive polymer cords (which became nonconductive because of swelling).

To determine if thin metal films could be vapor-deposited directly onto the plastic surface and aluminum pads of the modified HF RFID tags, a mask with a hole to expose the IC bypass pads for vapor deposition was placed over the RFID tag/antenna. When the RFID tag was vapor-deposited with copper, the tag became unreadable (the IC bypass formed by the copper film was conductive and adherent to the pads/plastic surface). The vapor-deposited copper films were determined (surface profilometer) to range from 0.7 to 1 micron in thickness. Figure 12 shows the modified HF RFID tag with the IC bypass completed by the vapor-deposited copper film.

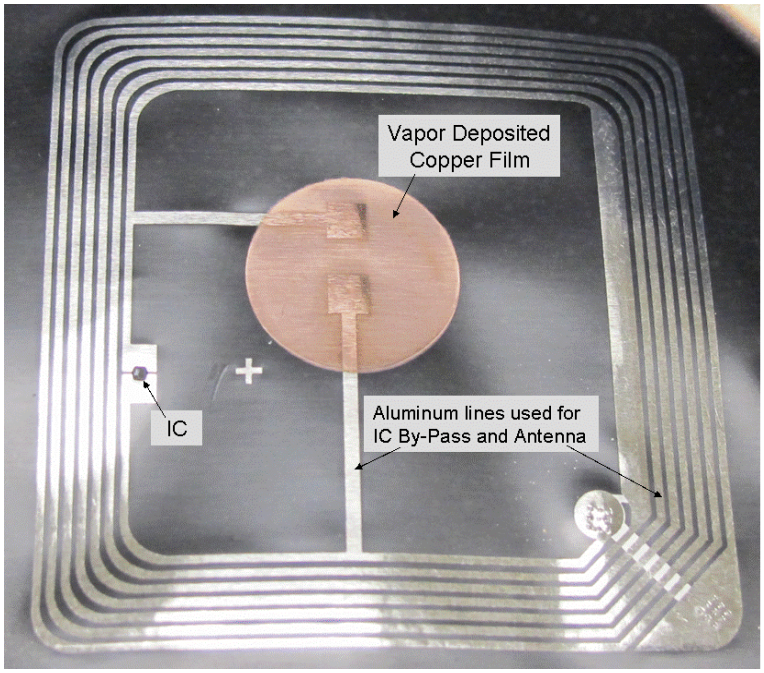

Figure 12. SMART Chemical Sensor Using a Vapor-Deposited Copper Film to Complete the IC Bypass

To initially evaluate the chemical sensitivities of the different vapor-deposited metal films, conductive (<10Ω) metal films of aluminum, copper, and tin were vapor-deposited onto microscope glass slides. Each glass slide was then broken into several smaller pieces to allow multiple tests with each metal film. The first chemical test was performed with hydrofluoric acid

(HFA) vapors in a laboratory chemical hood (HFA vapors are generated by certain cross-linked wiring insulations). Sections of the metal-deposited glass slides were placed on top of small cups, which contained a few drops of aqueous concentrated HFA (metal films exposed to HF vapor in headspace above acid drops). Three sections from each metal-coated glass slide were used in this initial study:

- The first section (new) was set aside (represents beginning metal film).
- The second section was placed for 5 minutes in the HF vapor, then was removed and rinsed in distilled water (any residual HFA acid/loose metal film was washed off).
- The third section was placed in HF vapor for 60 minutes, then was removed and rinsed in distilled water.

The three sections of coated-glass films shown in figure 13 demonstrate that the chemical reactivities of the tin, aluminum, and copper metal films are quite different for HFA vapor.

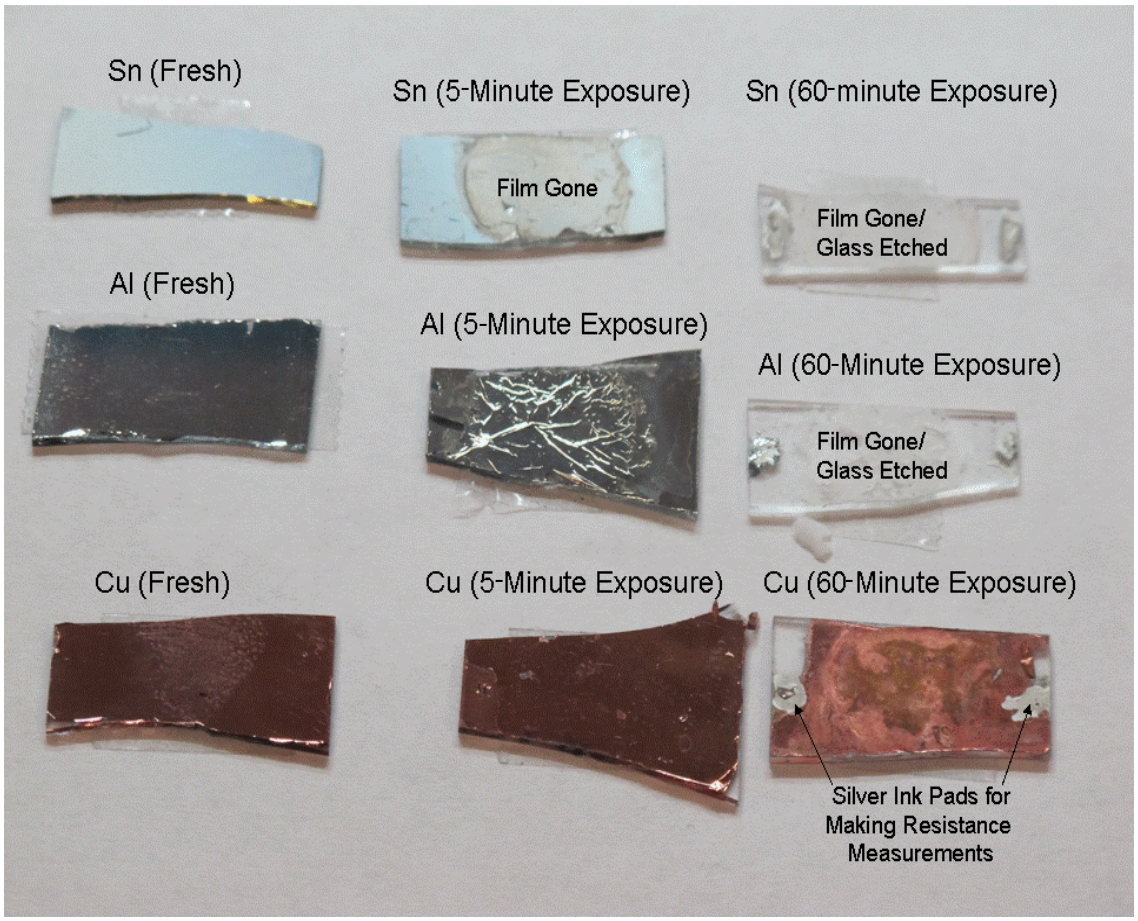

Al = aluminum, Cu = copper, Sn = tin

Figure 13. Glass Slide Pieces With Tin, Aluminum, and Copper Metal Films Before and After Exposure to HFA Vapors

The tin coating (slight oxidation gives it a whitish appearance) in figure 13 is greatly reduced visually after only 5 minutes of HFA vapor exposure (resistance increased from 2 Ω to 2 KΩ; RFID tag readable but range reduced) and is completely removed/glass-surface-etched after 60 minutes (resistance >6 MΩ: open circuit; HF tag readable). Although the appearance of the aluminum coating changed dramatically after 5 minutes of HFA vapor exposure, the film's resistance remained ~1 Ω, so that readability of an associated RFID tag would be unaffected. Even after 60 minutes, the aluminum coating still remained intact (resistance ~1 KΩ) until the aluminum slide was submerged in water, which caused the entire exposed film to fall off the slide, revealing the etched-glass surface (resistance >6 MΩ; open circuit, HF tag readable). In contrast to the tin and aluminum films, the copper films in figure 13 remained intact (resistance <20 Ω; closed circuit, HF tag unreadable) regardless of the exposure time to HFA and rinsing with distilled water.

To expand on the initial research, additional metal-coated glass slides were prepared with silver and nickel; then the different metal-coated slide pieces were exposed to drops of the following aqueous solutions to produce the reacted metal films shown in figure 14:

- Basic (5% potassium hydroxide (KOH)) solution
- Acidic (10% acetic acid and 1% hydrochloric acid (HCl)) solution
- Salt (sodium chloride (NaCl) and potassium acetate (KAc)) solution

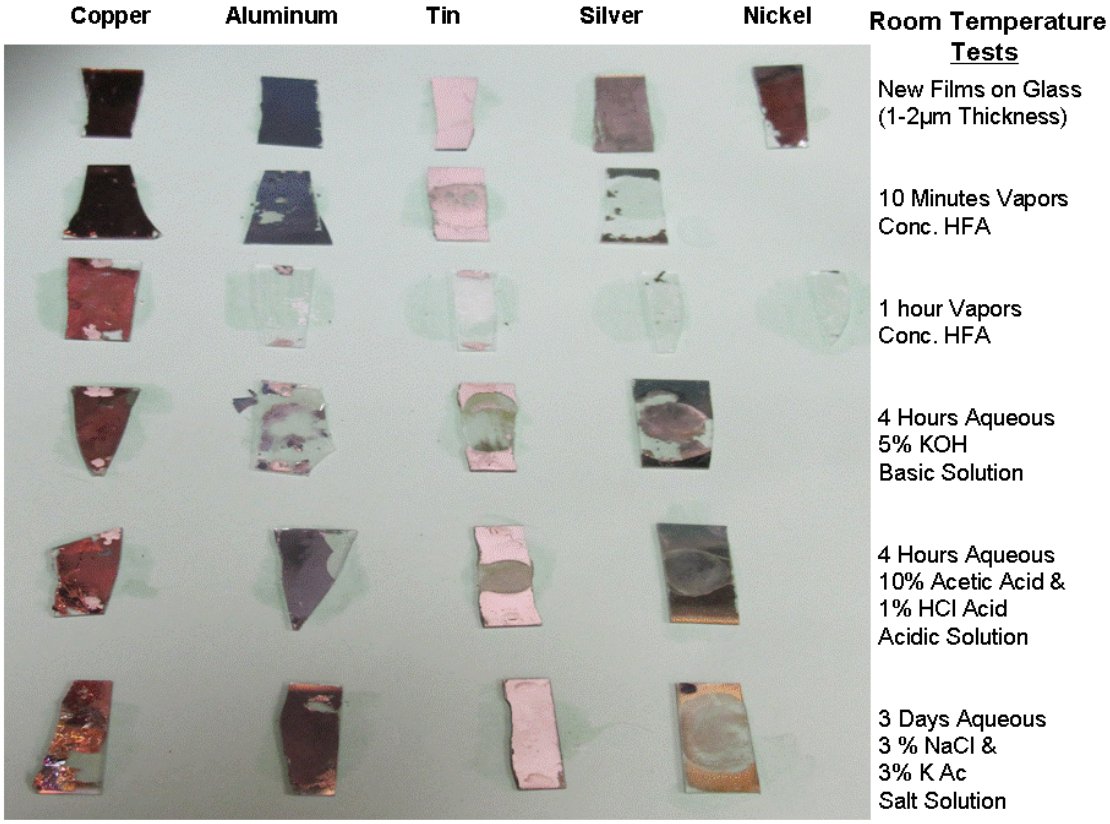

Figure 14. Glass Slide Pieces With Different Metal Films Before and After Exposure to Corrosive Vapors and Aqueous Solutions

The results in figure 14 show that copper is resistant to most of the corrosive environments, except for the aqueous salt solution (an NaCl and KAc combination was used to simulate EWIS exposure to runway deicer solution). As opposed to the copper film, the silver films appeared to be sensitive to all of the corrosive environments. A significant amount of the sensitivity was attributed to poor adherence of the silver film because the exposed films remained conductive and appeared unaffected until water washing to remove the contaminants caused large silver flakes to release from the glass surface.

The tin-deposited films (tin oxidized during the vapor deposition, resulting in the white surface), which reacted very quickly with the HFA vapors, required 4-hour exposures to the basic and acidic solutions (simulated cleaners) before becoming nonconductive (the removed portion of film shows the size of the solution drop in figure 14). As opposed to the copper film, the tin film was resistant to the aqueous salt solution even after 3 days/repeated drops.

As expected, the aluminum film corroded by the HFA vapor was also severely corroded by the basic solution. Surprisingly, the aluminum film was resistant to the acidic and salt solutions. Although the aluminum films had a mirror finish in the above picture, the films may have had a thin, protective oxide layer. Because of poor adherence to the glass surface, only one test was run with the nickel film, which was rapidly degraded by the HFA vapors.

To produce SMART chemical sensors with different chemical sensitivities, the metals shown in figure 14 were vapor-deposited onto the surface/IC bypass pads of modified HF RFID tags. In each case, the metals formed a conductive, adherent film similar to the copper film shown in figure 12 (although conductive, the tin film had a white, oxide outer layer).

In agreement with the metal film on glass slide results, the SMART chemical sensors with the tin and aluminum metal films completing the IC bypasses became readable (metal film removed) within 15 minutes of exposure to the HFA vapor. Additionally, the aluminum lines of the IC bypass were attacked by the HFA vapor (areas of lines with dull finish in figure 15).

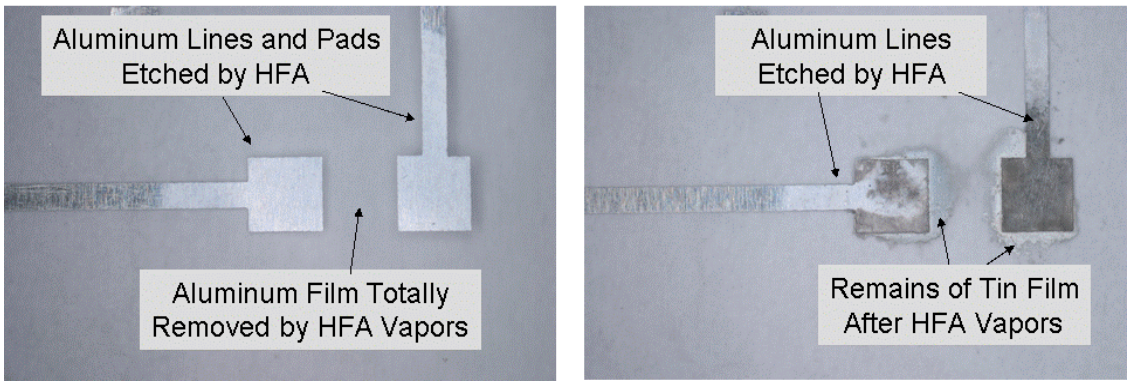

Figure 15. SMART Chemical Sensors Completed by Aluminum and Tin Metal Films After Exposure to HFA Vapors

Since the aluminum lines were being attacked by the HFA vapors, the IC bypass of a SMART chemical sensor was completed with silver epoxy (resistant to HFA) and the HFA vapor

experiment was repeated. Since the aluminum bypass lines were much thicker (50 microns) than the deposited films (1 micron), the sensor required 60 minutes of exposure to the HFA vapors before becoming readable (silver epoxy bypass was intact and aluminum line was corroded/broken, as shown in figure 16).

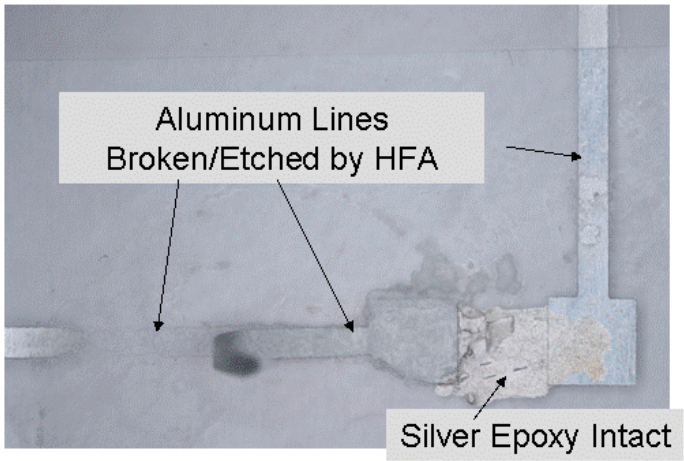

Figure 16. SMART Chemical Sensor Completed With Silver Epoxy Line After Exposure to HFA Vapors

As opposed to the silver film on the glass slide results, the HFA vapors did not remove the silver film from the plastic surface of the SMART chemical sensor (the RFID tag remained unreadable after 1 hour of exposure). In contrast to the plastic surface in figure 17, the silver was removed from the aluminum lines/pads (etched) during the 1-hour test (copper had similar results, indicating that galvanic corrosion between dissimilar metals could be used to increase the corrosion rate of the IC bypass).

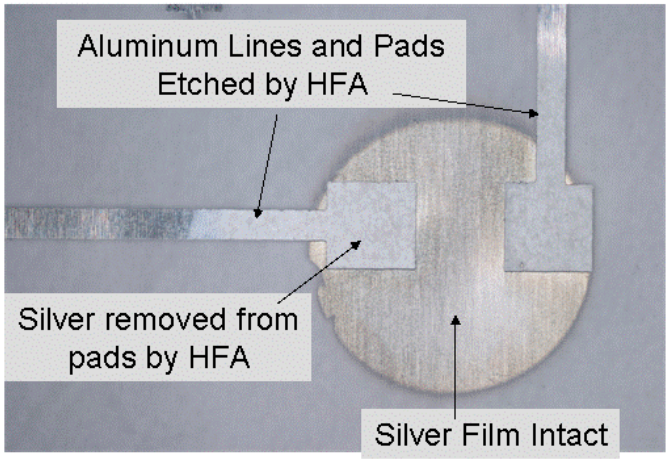

Figure 17. SMART Chemical Sensor Completed With Silver Metal Film After Exposure to HFA Vapors

These results indicate that the sensitivity of the SMART sensor can be adjusted by levels of magnitude by the thickness of the metal film used to complete the IC bypass, and that the chemical species to be detected by the SMART sensor can be selected based on the type of metal(s) selected to complete the bypass.

The SMART chemical sensors with either aluminum or tin (possibly nickel) completing the IC bypass would be well-suited for detecting HFA vapors and other fluorinated vapors (combustion gases of wires with fluorinated insulation) in EWIS compartments. The reactivity/thickness of the vapor-deposited metal films would dictate the sensitivities of the RFID sensors to different concentrations of corrosive vapors. The usefulness of the copper film for detecting HFA vapors would depend on galvanic corrosion at the copper/aluminum interface on the RFID surface (see figure 16 and previous research [4] that indicated corrosion was more rapid at the copper/aluminum interface of copper-clad aluminum wiring than in the isolated aluminum wiring core).

In the case of corrosive liquids (see figure 14), SMART chemical sensors with tin completing the IC bypass would be well-suited for detecting basic or acidic liquids, such as toilet cleaners. The results are less conclusive for the aluminum films since they reacted with basic solutions, but not with acidic or salt solutions (a possible explanation is that oxide layers are protecting the aluminum films from acidic or salt attack). In contrast to the tin and aluminum results, SMART corrosion sensors with the vapor-deposited copper film completing the IC bypass have potential for detecting corrosion by deicer contamination for aircraft EWIS components exposed to a runway environment.

In addition to corrosive vapors or liquids, SMART chemical sensors could be designed to detect combustive liquids (fuel, lubricating oil, grease, etc.) leaking onto aircraft EWIS. To detect the leaking liquids, a conductive silicone rubber cord (which contains copper and silver particles) was used to complete the IC bypass, as shown in figure 18.

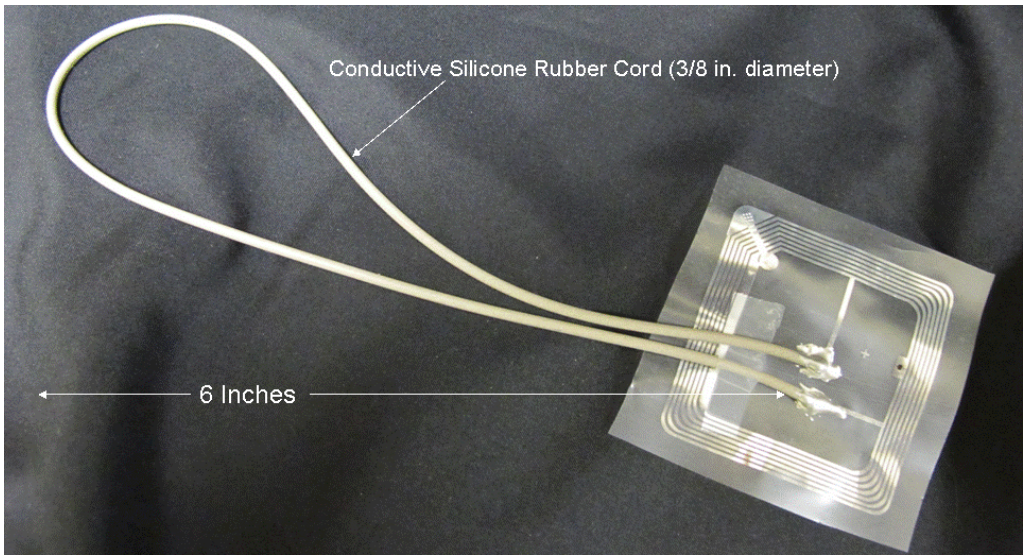

Figure 18. SMART Chemical Sensor Using a Conductive Silicone Rubber Cord to Complete the IC Bypass

As opposed to the SMART chemical sensors with metal films, the silicone rubber cord changes from conductive to nonconductive due to swelling of the rubber matrix. Once the cord is cleared of the leaking fluid, it becomes conductive again (reusable sensor). Because of the high conductivity of the silicone rubber cord (~10Ω per foot), a 100-foot length of cable can be monitored by one RFID tag, allowing it to be situated in a location easily accessible by maintenance personnel (the back of the access panel).

A SMART chemical sensor capable of detecting water leaking onto aircraft EWIS was designed by using a water-soluble polymer solution (polyvinyl alcohol [1]) to coat the plastic substrate between the aluminum pads of the modified RFID tag. A silver ink pen was then used to draw a thin conductive line on top of the water-soluble film to electrically connect the aluminum pads of the IC bypass. When drops of water were allowed to run across the coated IC bypass, the modified RFID became readable after about 10 minutes (the polymer coating dissolved, causing the conductive silver line to break).

Consequently, the SMART chemical sensor can be designed to detect a wide range of environments (corrosive, combustible, wet, etc.) capable of leading to aircraft EWIS malfunctions. The selectivity and sensitivity of the chemical sensor to the chemical species to be detected is totally dependent on the composition and thickness of the material used to complete the IC bypass.

5. SMART IMPACT SENSOR.

The task was initiated with a literature search to identify force-sensitive switches suitable for use as the triggering mechanism in a SMART impact sensor. Several miniature sensors were identified during the literature search and at sensor-based conferences [3 and 5]. However, all of the identified commercial/prototype sensors required power (SMART sensor is passive) or were determined to be unsuitable for the aircraft environment [6].

The only passive g-force switches deemed suitable for use in the SMART impact sensors were accelerometers based on a ball/spring combination or a permanent magnet (selected to hold a steel ball in place up to a predetermined force of impact). Because of the high cost/low availability of the permanent magnet sensors, ball/spring accelerometers were pursued for this work. However, most of the switches were normally open (required redesign of the modified RFID tag) and were above $300 (unsuitable for routine use). Therefore, a small, normally closed, 2 g-force switch used in model rockets ($17) was obtained. The small switch was encased in epoxy and then cross-sectioned (as shown in figure 19) to better view its ball/spring mechanism.

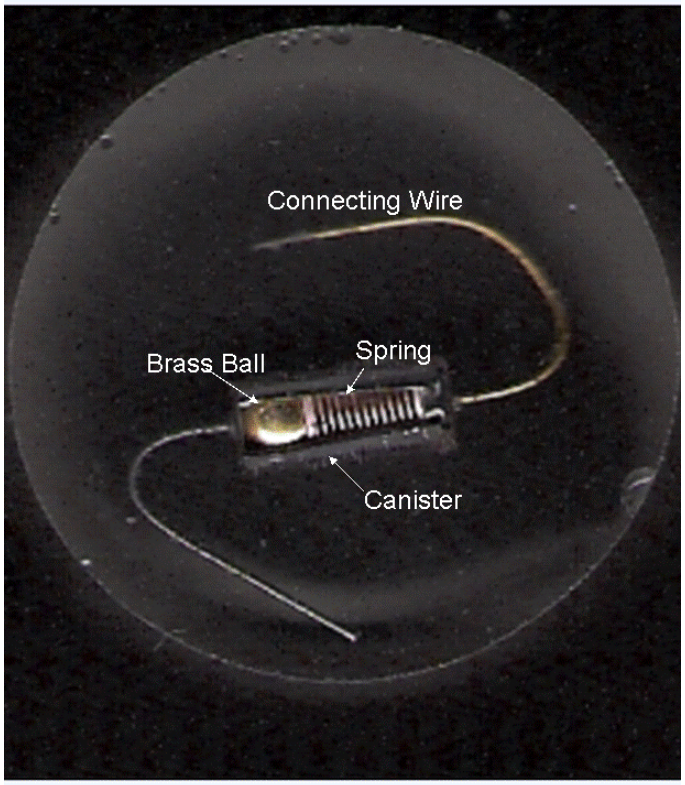

Figure 19. Cross-Sectioned Normally Closed G-Switch

The normally closed g-force switch is a small metal canister containing a metal ball and spring. As the switch experiences acceleration in the direction of the spring, the ball compresses the spring, electrically opening the switch circuit. However, once the acceleration ends, the spring reexpands, the ball returns to its starting position, and the g-switch becomes electrically closed again. Consequently, the g-switch in figure 19 would be unsuitable for use in a SMART impact sensor because the switch would always be closed (RFID tag unreadable) during maintenance actions on the ground, regardless of the acceleration/impacts experienced by the sensor (unsupported wire) during flight.

Commercial impact shipping sensors (IOG Products, Chatsworth, CA) that monitor bi-directional, two-axis accelerations were then obtained (available in the 2 to 300 g range in steps of 1 g). The shipping sensor is available in two set ups: one-time use and reusable. The one-time use has a permanent cover while the cover of the multiple use sensor is removable so the sensor can be reset for additional uses. Each type of shipping sensor consists of two sets of steel ball/spring combinations with a steel ball at each end of each spring (acceleration is measured in either direction along the selected axis) and the balls are held in place (depression in plastic flange) until the preset acceleration exceeds the force exerted by the spring. Figure 20 shows a single-use sensor with the lid cut off.

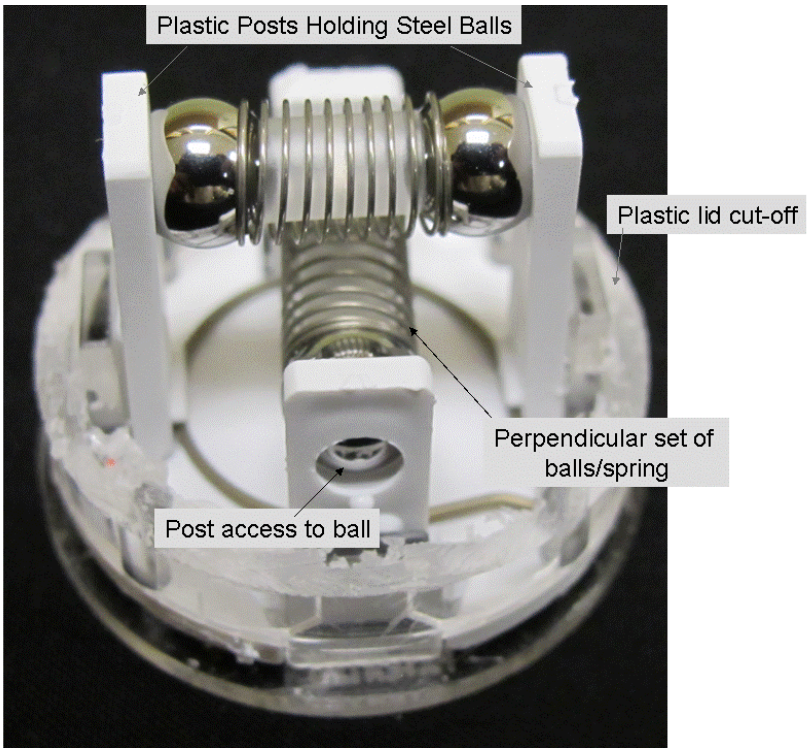

Figure 20. One-Time Use Shipping Sensor Based on Spring/Ball Concept

When either ball compresses the spring, both balls drop out of their depressions and the spring/ball combination falls apart (figure 21), providing a visual indication that the monitored package had been dropped (preset acceleration exceeded).

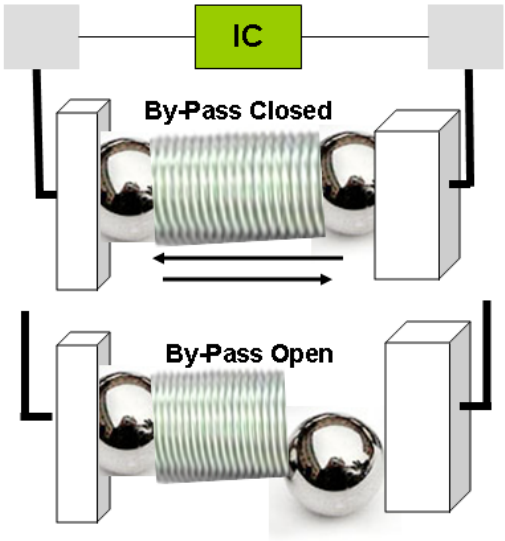

Figure 21. Ball/Spring Combination Falling Apart After Acceleration

Electrical connections were added to the the SMART impact sensor shipping setup to complete the IC bypass, as shown in figure 21. However, initial measurements showed that the electrical contact between the spring and each steel ball was poor (contact resistance >10 KΩ), making the setup unsuitable for the SMART impact sensor (which requires bypass resistance to be less than 1 KΩ (tables 2 and 3)). Using silver epoxy to connect the balls to the spring reduced the contact resistance to below 10Ω and the overall resistance of the ball/spring/ball combination to below 50Ω, making the setup suitable for incorporation into the bypass of a SMART impact sensor.

To test the accuracy of the commercial ball/spring accelerometer (with/without the silver epoxy) and to determine the g-forces experienced by an unsupported wire harness hitting up against a structure, the simple experiment setup in figure 22 was used.

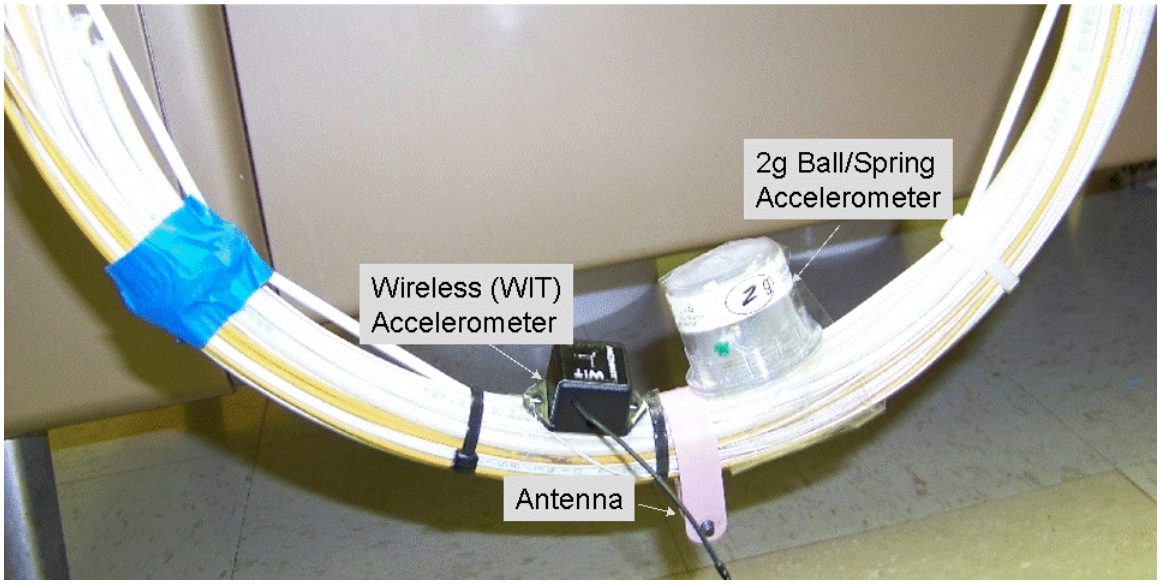

Figure 22. Unsupported Wire Bundle With Wireless and Ball/Spring Accelerometers Attached for Monitoring Structure Impacts

The 3-foot-long wire bundle shown in figure 22 was constructed from a wide variety of 12- to 20-gauge aircraft wires. The wire bundle was then attached to a cord with tape (see the blue wrap in figure 22) and hung from a desk to simulate an unsupported wire bundle swinging against an aircraft structure. A commercial powered accelerometer (Monnit Corporation, Midvale, UT: WIT™ model (~$350)) was attached to the wire bundle to measure the forces experienced by the wire bundle each time it was shaken and/or swung up against the desk with different ball spring accelerometers attached (the reusable 2-g accelerometer is shown in figure 22). The WIT accelerometer is 3-axis and wireless, sending out a signal whenever a preset g-force (1 to 8 g) has been exceeded. The threshold of the ball/spring accelerometers tested in this study ranged from 2 to 100 g. Table 4 shows the data generated by the WIT and ball/spring accelerometers while the wiring bundle was shaken and swung up against the desk along the XY and Z axes.

Table 4. Data Generated by Different Accelerometers Attached to Unsupported Wire Bundle During Shaking and Impact Motions

G Threshold	XY swing	Z swing	XY force hit	Z force hit
WIT Accelerometer Setting Exceeded				
1	no	no	yes	yes
2	no	no	yes	yes
4	no	no	yes	yes
6	no	no	yes	yes
8	no	no	yes	yes
Ball/Spring Accelerometer Setting Exceeded				
2	no	no	yes	yes
4	no	no	yes	yes
6	no	no	yes	yes
8	no	no	yes	yes
10	no	no	yes	yes
20	no	no	no	no
50	no	no	no	no
100	no	no	no	no

The data in table 4 indicate that, when the wire bundle was swung along the XY axis or shaken in the Z direction, the g-forces experienced by the unsupported wiring were below 1 g. However, when the wire bundle was swung up against the desk at different speeds (XY force hit) or dropped on a surface (Z-force hit), much higher g-forces were generated, as indicated by the WIT accelerometer data. Whenever the preset acceleration of the WIT accelerometer was exceeded, the corresponding ball/spring accelerometer was also exceeded (with or without silver epoxy). Although this simple experiment is not conclusive, it does indicate that an accelerometer with a g-force threshold in the range of 2 to 4 g, not being triggered by the accelerations of supported wires during normal flight, would be triggered by unsupported wires swinging against structures.

In addition to the accelerometer work, tilt sensors were also investigated as a means to detect unsupported wire harnesses. The tilt sensors consist of a small brass cylinder containing two small brass balls, one loose and the other attached to the bottom of the cylinder. When the cylinder is vertical, the brass balls lay in contact with each other, forming a closed circuit. When the cylinder is tilted past 45 degrees, the balls separate, breaking the electrical circuit. If a tilt sensor is incorporated into the IC bypass of the modified HF RFID tag (figure 23), the modified RFID tag cannot be read as long as the sensor remains vertical (wire harness supported). However, if the tilt sensor moves past 45 degrees (horizontal/inverted), the IC bypass opens and the modified RFID tag can be read (wire harness unsupported/swinging).

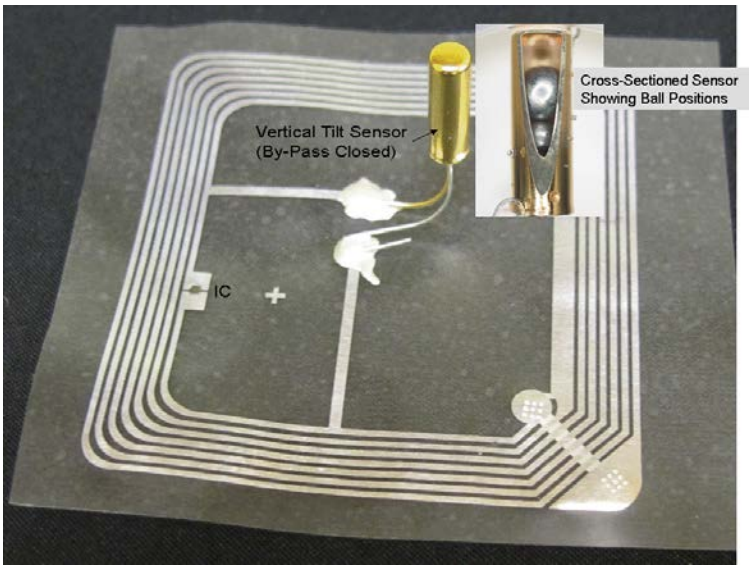

Figure 23. SMART Impact Sensor Using a Tilt Sensor (Cross-Section Insert) to Complete the IC Bypass

In addition to the accelerometers and tilt sensors studied for use in a SMART impact sensor, breakable circuits (conductive traces on thin, alumina/glass slides) could be placed on such surfaces as fuel tanks, hydraulic lines, where the component being struck is of higher priority/risk than the unsupported wiring harness. Laboratory studies using breakable circuits found that 750 to 800 grams were required to break scribed alumina slides (figure 24), which is equal to a lightweight wiring harness making a 5-g impact, well within the test parameters of the wire harness (figure 22 and table 4).

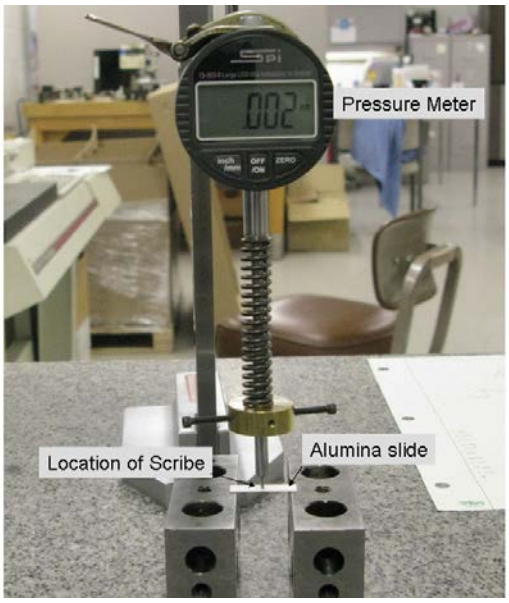

Figure 24. Experimental Setup for Determining Weight Required to Break Scribed Alumina Slide

The initial results for the SMART impact sensor indicate that different designs have potential for monitoring aircraft EWIS and surrounding systems. Although the ball/spring mechanism of the shipping impact sensor performed well in the laboratory experiments, a miniaturized version of the mechanism is needed for use in actual aircraft environments. Also, more information is needed to specify the triggering g-force level(s) of the SMART impact sensor design for both the ball/spring and breakable circuit mechanisms. The SMART impact sensor based on the tilt sensor is basically ready for further testing on aircraft EWIS, where loss of support is more critical than force of impact.

6. SMART POWER SENSOR.

Compared to the other SMART sensors, the SMART power sensor received minimal attention during this project. The first SMART power sensor was constructed by completing the IC bypass with a reed switch, as shown in figure 25.

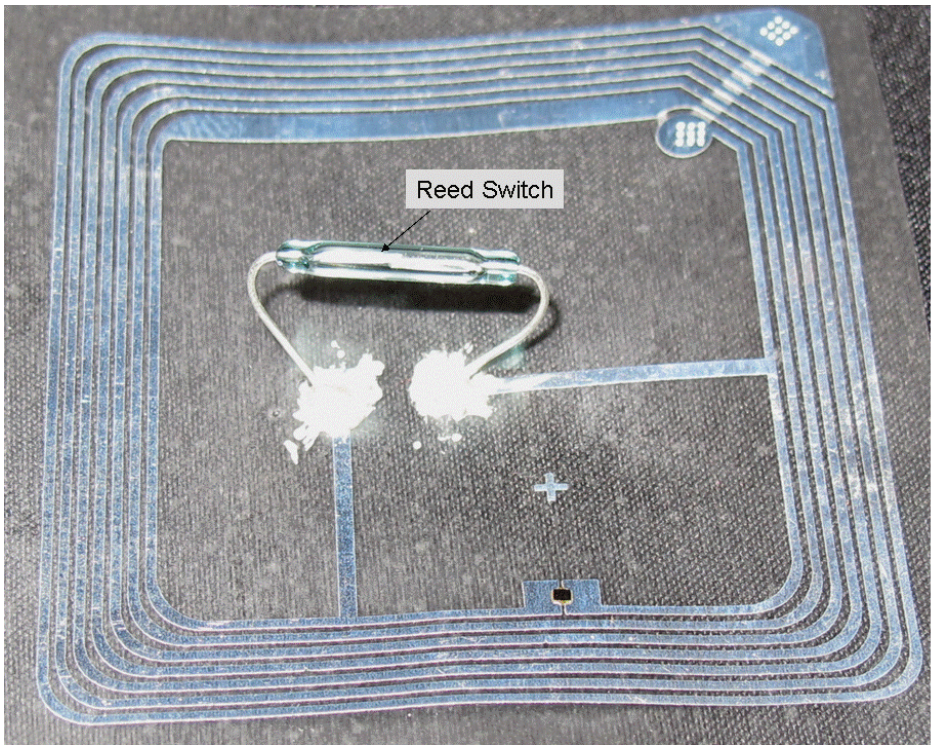

Figure 25. SMART Power Sensor Using a Reed Switch to Complete the IC Bypass

The concept is that the SMART power sensor is positioned near the EWIS component of interest so that, when power is applied, the generated magnetic field (generated by power, component, or inductively-coupled electromagnet) causes the reed switch to change state.

If a normally closed or normally open reed switch is used, then the generated magnetic field opens (the RFID tag activates) or closes (the RFID tag deactivates) the reed switch, respectively, when power is applied to the component of interest. In this manner, the SMART power sensor

can be used to determine if a system failure is due to lack of power (an EWIS breakage) or component failure.

Another design of the SMART power sensor could be used to detect arcing events and other power surges during flight. The idea is to use a normally closed light-sensitive (photocell) or radio frequency-sensitive element to complete the IC bypass so that, when the arcing event occurs, the energy-sensitive element permanently opens, activating the modified RFID tag for maintenance personnel to detect at a later time.

7. SMART CRACK SENSOR.

Because the concept of a SMART crack sensor was researched extensively in previous work [1], minimum research was performed on the concept (crack sensors were included in SMART clamp and impact sensor designs). As compared to the other SMART sensors, the design of the trace circuit used to complete the IC bypass of the modified RFID tag is completely dependent on the surface and component to be monitored. If the sensor is to detect when a component (such as a clamp) breaks, then the trace is simply an adherent, conductive line that breaks on component damage/breakage. However, if the crack sensor is to detect fatigue cracks and other hairline surface features, then the trace composition has to match that of the surface so that the trace fails at the same rate as the monitored component. If predictive capabilities are required, then the trace completing the IC bypass could be designed to fatigue at a higher rate than the component so that the SMART crack sensor would activate when the component still has residual life remaining.

8. CONCLUSIONS.

This report details the results of a 12-month grant research program performed by the University of Dayton Research Institute (UDRI) to improve the reliability and intelligence of aircraft electrical wiring interconnect systems (EWIS) through improved malfunction detection. This initial research was performed to develop radiofrequency identification (RFID) tag based sensors that are activated by abnormal operating conditions prior to EWIS or associated component failure. Three different types of RFID tags were investigated: 125 KHz (low frequency (LF)), 13.56 MHz (high frequency (HF)), and 902 MHz (ultrahigh frequency (UHF)). The LF and HF tags have much shorter read ranges (few inches) than the UHF tags (greater than 10m). However, the LF and HF tags transmit through conductive materials such as carbon tap. During this grant, UDRI composite group developed conductive lines made from an epoxy resin/carbon nanofiber mixture applied to a composite surface for making manual resistance measurements (UDRI received a US patent on the concept of conductive line measurements in April 2011).

This report only covers this initial study of RFIDs as sensors on aircraft. After the successful completion of this grant, the UDRI RFID sensor work will continue on a 3-year FAA contract DTFACT-12-C-00009. The final results and conclusions will be published at the completion of the contract.

9. REFERENCES.

1. Kauffman, R., FAA Grant 08-G-001, "Development of Technologies to Improve the Reliability and Intelligence of Aircraft Electrical Wire and Interconnect Systems," Awarded June 2009 Monthly Progress Reports (Final report June 2010)

2. Kauffman, R. and Wolf, J.D., U.S. Patent Application 20100295694, "SMART Aerospace Structures," November 25, 2010.

3. Kauffman, R., "Status and Motion Activated Radiofrequency Tag (SMART) Sensors," NASA Tech Briefs SENSORS Tech Forum, Boston, Massachusetts, October 10-13, 2011.

4. Kauffman, R., et al., Final Report for FAA Grant: 06-G-015, "Development of Technologies to Monitor and Extend the Performance of the Electrical Wire and Interconnect Systems of Aging Aircraft," October 2007.

5. Kauffman, R. and Toomb, M., (American Thermal Instruments), "What You Need To Know About Status Motion Activated Radiofrequency Tag (SMART) Sensors," Sensors in Design, Embedded Systems Conference, San Jose, California, March 28-29, 2012.

6. Jean, D., "Integrated MEMS Mechanical Shock Sensor," Proceedings of the 48th annual NDIA Fuze Conference, Charlotte, North Carolina, April 26-28, 2004.